

Formulation, characterization, and optimization of aripiprazole-loaded lyotropic liquid crystalline nanoparticle for sustained release and better encapsulation efficiency against psychosis disorder

Mardhiah Maslizan¹, Lai Yip Khen¹, N. Idayu Zahid², Shah Christirani Azhar³, Intan Diana Mat Azmi^{1,3*}

¹ Department of Chemistry, Faculty of Science, Universiti Putra Malaysia, 43400 UPM Serdang, Selangor Darul Ehsan, Malaysia

² Centre for Fundamental and Frontier Sciences in Nanostructure Self-Assembly, Department of Chemistry, Faculty of Science, Universiti Malaya, 50603 Kuala Lumpur, Malaysia

³ Centre of Foundation Studies for Agricultural Science, Department of Chemistry, Faculty of Science, Universiti Putra Malaysia, 43400 UPM Serdang, Selangor Darul Ehsan, Malaysia

ABSTRACT

Lyotropic liquid crystalline nanoparticles (LLCNPs) have recently received much attention in the application of drug delivery systems, due to their ordered and versatile internal nanostructures that are considered as a key factor in improving loading efficiency of various poorly soluble therapeutic agents. To take advantage on their unique well-defined and flexible internal nanostructures, aripiprazole-loaded LLCNPs consisted of a binary mixture of soy phosphatidylcholine (SPC) and citric acid ester of monoglyceride (citrem) were developed in this study. Despite exhibiting low aqueous solubility which lead to difficulties in formulation, aripiprazole, a class of psychotropic drug called atypical anti-psychotics has been used in the treatment of schizophrenia and bipolar disorder with few side effects. The utmost interest in this study is to explore the potential of LLCNPs in improving the percentage of encapsulation efficiency (EE%) of aripiprazole, their effect on the internal nanostructure of LLCNPs mesophases as well as the drug release performance from LLCNPs. The particle size of drug-loaded LLCNPs produced was in the range of 161–186 nm, with polydispersity index (PDI) between 0.11–0.16, and negative zeta potential of -21.5 to -23.8 mV. Small-angle X-ray scattering (SAXS) measurements indicated that the internal nanostructures of LLCNPs are of inverse hexagonal (H₂) with a negligible difference in the lattice parameter before and after drug loading. Transmission electron microscopy (TEM) was used to observe the morphology and overall size distribution of drug-free and drug-loaded nanodispersions, which supported both SAXS and particles size findings. Differential scanning calorimetry (DSC) and Fourier transform infrared (FTIR) spectroscopy demonstrated that aripiprazole interacted physically with binary mixture of citrem/SPC within the nanodispersions. Moreover, the results showed that aripiprazole was successfully encapsulated into LLCNPs nanoparticles, where the EE% was all above 92%. These LLCNPs were not only have a high EE% value, but also exhibited a sustained release performance of aripiprazole with the release capacity of around 97% up to 96 h. From the current study, the potential use of LLCNPs as a promising nanocarrier for aripiprazole delivery is anticipated to improve the pharmacokinetics of this drug whilst enduring the internal nanostructural stability of the LLCNPs upon exposure to physiological environment.

Keywords: Liquid crystalline, Nanoparticles, Aripiprazole, Drug release.

OPEN ACCESS

Received: July 17, 2021
Revised: January 02, 2022
Accepted: March 24, 2022

Corresponding Author:
 Intan Diana Mat Azmi
intandiana@upm.edu.my

 **Copyright:** The Author(s). This is an open access article distributed under the terms of the [Creative Commons Attribution License \(CC BY 4.0\)](https://creativecommons.org/licenses/by/4.0/), which permits unrestricted distribution provided the original author and source are cited.

Publisher:
[Chaoyang University of Technology](https://www.cup.edu.my/)
 ISSN: 1727-2394 (Print)
 ISSN: 1727-7841 (Online)

1. INTRODUCTION

The agriculture sector in Malaysia contributed RM96.0 billion to the Gross Domestic Product (GDP) in 2017. Oil palm was a major contributor to the GDP of the agriculture sector at 46.6% followed by other agriculture sectors (18.6%), livestock (11.4%), fishing (10.5%), rubber (7.3%) and forestry products (5.6%) (Department of Statistics Malaysia, 2018). There has been an increased usage of chemical fertilizer as it helps in growing crops on the economic scale. Chemical fertilizers (inorganic) are widely used in modern agriculture to amend nutrient deficiencies; to provide high levels of nutrition, which aid plants in withstanding stress conditions; to maintain optimum soil fertility and improved crop quality.

The drug solubility and its desired concentration in systemic circulation are some of the important criteria that need to be achieved in order to have a good therapeutic outcome, which would improve the success rate in the pharmaceutical development (Savjani et al., 2012). It turns out that most of the drug candidates are having disadvantage of poor water solubility which renders a low potential for their bioavailability (William et al., 2013; Kalepu and Nekkanti, 2015). Aripiprazole, an anti-psychotic drug that is being used to treat schizophrenia and bipolar disorder, also showed poor aqueous solubility which limits its clinical use (Kumar et al., 2020).

Many attempts have been made to improve the solubility of aripiprazole including via nanoprecipitation or nanosuspension of the drug, formation of complexes with cyclodextrin as well as solubilization in different type of oils and lipids (Xu et al., 2012; Badr-Eldin et al., 2013). The previous findings of a dramatically higher percentage of cases reported with the depot formulation suggests that the risk of developing impulse control disorders (ICDs) while taking aripiprazole may be dosage dependent (Lertxundi et al., 2018). Another technique is by incorporating aripiprazole into lyotropic liquid crystalline nanoparticles (LLCNPs) which were described to have good tolerability, minimal cytotoxic effects, and could provide an alternative solution for poorly soluble drug therapeutics without altering the molecular structure (Akbarzadeh et al., 2013; Cerpnjak et al., 2013; Kalepu and Nekkanti, 2015).

LLCNPs are a promising drug delivery mechanism with the ability of loading pharmaceutical molecules of any polarity including proteins, peptides as well as nucleic acids (Krishna Sailaja et al., 2011; Asha Spandana et al., 2020). Because of their biocompatible and biodegradable features, stability, nontoxicity, potential to improve safety, effectiveness, and ability to penetrate across physiological barriers, LLCNPs have received a lot of interest in drug delivery research (Chountoulesi et al., 2018; Dutta et al., 2018; Huang and Gui, 2018; Tan et al., 2018; Chountoulesi et al., 2020; Maslizan et al., 2021; Yaghmur and Mu, 2021). Nanostructured liquid crystals, like liposomes (internal lamellar phase), cubosomes (internal bicontinuous cubic

phase), and hexosomes (internal hexagonal phase), can be formulated by dispersing these structures into the aqueous medium with the presence of suitable stabilizers, e.g. the citric acid esters of monoglycerides (citrem) (Spicer, 2004; Bhosale et al., 2013).

Amphiphilic lipids such as phospholipids, monoglycerides and glycolipids are the common lipids used in LLCNPs nanodispersion to form the nanocarrier (Akbarzadeh et al., 2013; Cerpnjak et al., 2013; Chime and Onyishi, 2013; Zhai et al., 2017). Depending on lipid compositions, pressure, pH, and temperature, these amphiphilic lipids will self-assemble in the aqueous medium into diverse nanostructures of LLCNPs (Guo et al., 2010; Thadanki et al., 2011; Chandrashekar, 2012; Huang and Gui, 2018). The highly ordered internal nanostructure of non-lamellar LLCNPs, especially the 3D-ordered cubosomes and the 2D-ordered hexosomes, offer advantages as a potential carrier for different types of therapeutic molecules while improving their solubility and stability from degradation (Bonate, 2011; Khani et al., 2016).

In this work, we present the possibility of using LLCNPs consisted of a binary lipid system citrem and phospholipid (soy phosphatidylcholine) at different lipid ratios, to improve the encapsulation efficiency of aripiprazole. Alongside with the important role of nanoformulation to tackle the solubility issue of aripiprazole, we have also addressed the potential of LLCNPs to offer a sustain release profile (long-acting therapy), which is important for non-adherence patients of anti-psychotropic medication. By understanding the physicochemical characteristic of the drug-free and drug-loaded LLCNPs as well as the drug release profile, the development of drug delivery system for anti-psychotic treatment will have higher chance to thrive as several studies on LLCNPs which have reported their ability to improve the aqueous solubility of hydrophobic medicines, high encapsulation efficiency, stability in biological fluids, drug retention capability, and tendency to transport drug across the blood brain barrier (Elezaby et al., 2017; Piazzini et al., 2020).

2. MATERIALS AND METHODS

2.1 Materials

Aripiprazole with purity 99.0% was purchased from Sigma Aldrich (Darmstadt, Germany). Soy phosphatidylcholine (SPC) with purity of 99.1% was purchased from Lipoid AG (Steinhausen, Switzerland). Grinsted® citrem LR10, which is a citric acid ester of monoglycerides made from sunflower oil, was received as a gift from Danisco A/S (Copenhagen, Denmark). Dulbecco's phosphate-buffered solution (PBS) was purchased from Thermo Scientific (Hampshire, UK).

2.2 Sample Preparation

2.2.1 Preparation of Drug-Free LLCNPs

Preparation of aqueous nano-dispersions involves a procedure that requires high-energy input (ultrasonication) (Azmi et al., 2016). Binary mixture of citrem/SPC was prepared at 1:1 ratio where the total lipid concentration was kept constant at 5% w/v. PBS was then added to the lipid mixtures to give 100% of total weight dispersion. The emulsification process was performed by means of ultrasonication (QSonica sonicator Q125, Newtown, USA) for 5 min in pulse mode (5 s pulses interrupted by 2 s breaks) at 20 and 50% of its maximum power until well-dispersed and stable milky solutions were obtained.

2.2.2 Preparation of Drug-Loaded LLCNPs

Aripiprazole-loaded citrem/SPC formulations were prepared via the ultrasonication method as well. Initially, aripiprazole at four different concentrations of 1.0, 2.0, 2.5, and 5.0 mg/mL with corresponding weights of 10, 20, 25, and 50 mg were added to already-prepared citrem/SPC nanodispersion (prepared as described in section 2.2.1) until achieving well-homogenized milky formulations. Subsequently, each formulation was dissolved in 10 mL of PBS/methanol (90:10 v/v) mixture with the aid of an ultrasonic bath on 37°C at 80 rpm to homogenize the drug formulation until well-dispersed and stable milky solutions were obtained (Piazzini et al., et al., 2020).

2.3 Characterization of Drug-Free and Drug-Loaded LLCNPs

2.3.1 Encapsulation Efficiency of Drug-Loaded LLCNPs

UV-Vis spectrophotometer (UV-1601, Shimadzu, Japan) was used to study the percentage of encapsulation efficiency (EE%) of aripiprazole-loaded LLCNPs. A series of standard aripiprazole solution concentrations in a range of 0.001 to 0.050 mg/mL was prepared and a calibration curve was plotted in order to determine the EE%. All measurements were based on x mg of free aripiprazole in 1 mL of solution taken from the sample solution, x mg/mL, to calculate back the total amount of free aripiprazole. Evenly distributed free aripiprazole in the solution was ensured by swirling the solution well before performing the measurement. A series of measurements was performed to ensure the stability of the encapsulated drug into the LLCNPs for five consecutive days. The EE% was calculated using the given formula in Equation 1 as follows:

$$\text{Encapsulation efficiency} = \frac{\text{Initial concentration of aripiprazole} - \text{concentration of free aripiprazole}}{\text{Initial concentration of aripiprazole}} \times 100\% \quad (1)$$

2.3.2 Particle Size, Zeta Potential, and Polydispersity Index

The particle size, zeta potential, and polydispersity index

(PDI) of the aripiprazole-loaded LLCNPs were determined by Zetasizer Nano ZS90 (Malvern Instruments Ltd, Malvern, UK) adopting the dynamic light scattering mechanism. This instrument was equipped with a 633 nm laser and 173 detection optics. To prevent multiple scattering negative impact, the aripiprazole-loaded LLCNPs (1 mL) have been diluted with PBS (9 mL) and the instrument was calibrated prior to the analysis at 25°C. Collection of data and analysis were conducted using Malvern DTS version 6.34 software. All the experiments were performed in triplicates and the average values were taken. The value of PBS solvent was used for the viscosity and refractive index.

2.3.3 Structural Characterization

Small-angle X-ray scattering (SAXS) technique was used to evaluate the liquid crystal phase and determine the important parameters of the structures obtained (Azmi et al., 2016; Saari et al., 2018). An analytical SAXS from SAXSpace (Anton Paar, Austria) was employed to characterize the dispersion scattering of the aripiprazole drug-loaded LLCNPs. The instrument was equipped with an X-ray tube (DX-Cu 12x0.45, SERFERT) emitting Cu-K α of wavelength, $\lambda = 0.1542$ nm at 50 mA and 40 kV. The Goebel-mirror focused and Kratky-slit collimated X-ray beam was line shaped (17 mm horizontal dimension at the sample) and scattered radiation from the samples (measured in the transmission mode) was recorded with a one dimensional MYTHEN-1k microstrip solid-state detector (Dectris Switzerland) within a q -range of 0.1 to 6.0/nm at a sample-to-detector distance of 317 mm, where q is the magnitude of the scattering vector applying the conversion q [1/nm] = $4\pi(\sin\theta)/\lambda$, with 2θ being the scattering angle with respect to the incident beam and λ the wavelength of the X-rays in nm. Silver behenate which has a periodicity of 5.84 nm (where d [nm] = $2\pi/q_1$ is the lamellar spacing obtained from the position of the first order reflection q_1) was used as standard. The sample (~60 μ L) was transferred onto a 1 mm quartz capillary cell holder and placed into the X-ray machine. The measurement was set to room temperature ($25.0 \pm 0.1^\circ\text{C}$) using a Peltier system (TCStage 150). An acquisition time of 15 min was applied for all measurements. The collected data were calibrated by normalizing the primary beam using SAXStreat software. The liquid crystal phases and their corresponding lattice parameters were analyzed using the SGI software (Space Group Indexing, V.03.2012).

2.3.4 Morphological Characterization

Transmission electron microscopy (TEM, JEOL JEM-2100, Japan) was used as a visualizing aid for the non-lamellar LLCNPs. Two samples were selected as representative i.e. drug-free and aripiprazole-loaded nanodispersions. Each nanodispersion was diluted 10 times with distilled water. A droplet of each diluted samples was then negatively stained with 1% aqueous solution of uranyl

acetate. The stained samples were placed on the 400-mesh carbon-coated copper grids and allowed to stand for 5 min at room temperature. Subsequently, the observation of the two samples were made with a transmission electron microscope at a voltage of 200 kV. The images were viewed with magnification between 20,000× to 50,000×.

2.3.5 Fourier Transform Infrared Spectroscopy (FTIR)

Fourier transform infrared spectra of aripiprazole, drug-free, and aripiprazole-loaded LLCNPs were evaluated to investigate the viable chemical interaction between aripiprazole and LLCNPs. The measurements were recorded on a Shimadzu IR Tracer-100 spectrometer (Japan) using the attenuated total reflectance (ATR) method. All data were obtained in the 4000–400 cm range, with a spectral resolution of 4/cm and collected after 4 scans.

2.3.6 Differential Scanning Calorimetry (DSC)

Differential scanning calorimetry measurements were performed to investigate the change in physical behavior and phase transition temperature of aripiprazole, SPC, drug-free, and aripiprazole-loaded LLCNPs and also to study the presence of interaction between the aripiprazole with the LLCNPs. The measurements were carried out on a Mettler Toledo DSC 822e calorimeter (Columbus, OH, USA). Indium was used as the standard sample to calibrate DSC runs. Samples of 5–15 mg were sealed in aluminum pans. The samples were heated at scanning rate of 10°C/min from 30 to 300°C under a nitrogen atmosphere. Heat flow-temperature curve, melting point and specific heat energy were analyzed using STARe Excellence Thermal Analysis software.

2.3.7 In Vitro Drug Release Profile of Aripiprazole-Loaded LLCNPs

In vitro drug release study was performed by a dialysis technique (Nethravani et al., 2014) shown in Fig. 1. A ratio of 1:1 (citrem: SPC) with aripiprazole concentration of 2.5 mg/mL was selected to be incorporated in the nanodispersion. Aripiprazole-loaded LLCNPs (5 mL) was placed in a dialysis bag (pore size ~12,000 Da) that was previously soaked for 2 h in the PBS (pH 7.4), cleaned and sealed at both ends. The whole dialysis bag containing 5 mL aripiprazole-loaded LLCNPs was placed into 250 mL PBS (pH 7.4) and shaken (80 rpm) at 37.0 ± 0.5°C. The water bath sonicator was covered to prevent the evaporation of release medium. At time intervals of 2, 20, 24, 48, 50, and 96 h, 4 mL aliquots were withdrawn from the medium followed replacement with an equivalent volume of fresh PBS solution in order to maintain constant volume throughout the experiment. The amount of the drug diffused was estimated from the samples at 254 nm using UV-vis spectrophotometer (UV-1601, Shimadzu, Japan). All the experiments were performed in triplicates and the average values were taken. The formula for determination of

cumulative percentage release of aripiprazole is given in Equations 2 and 3 as follows:

$$\text{Amount of drug released (mg/mL)} = \frac{\text{Concentration} \times \text{Dissolution bath volume} \times \text{Dilution factor}}{1000} \quad (2)$$

$$\text{Cumulative percentage release (\%)} = \frac{\text{Volume of sample withdrawn (mL)}}{\text{Bath volume (v)}} \times P(t-1) + P_t \quad (3)$$

where P_t = Percentage release at time t

where $P(t-1)$ = Percentage release previous to ' t '

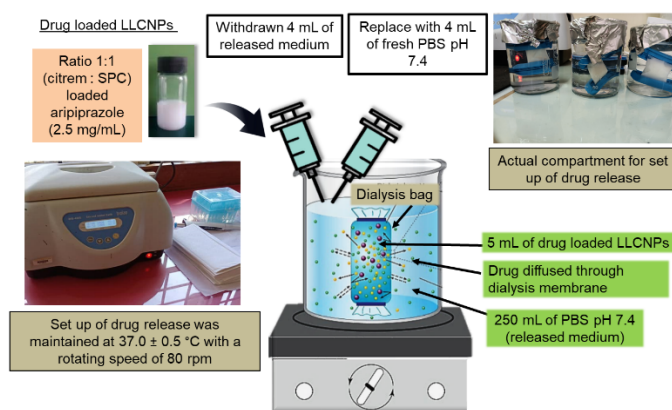


Fig. 1. *In vitro* drug release test method using dialysis technique. The appearance of drug-free concentration in the release medium is the result of diffusion from the drug-loaded nanoparticle followed by diffusion across the dialysis membrane was measured using UV-vis spectrophotometer (Modi and Anderson, 2013).

2.3.8 Statistical Analysis

All data were expressed as average ± SD (standard deviation) unless particularly outlined. The data were compared using one sample *t*-test for independent sample and one-way analysis of variance (ANOVA) for multiple group comparison procedure. All statistical comparisons were calculated using SPSS software version 16.0 (SPSS Inc., Chicago, IL). A *p*-value < 0.05 was considered statistically significant.

3. RESULTS AND DISCUSSION

3.1 Encapsulation Efficiency of Drug-Loaded LLCNPs

The encapsulation efficiency (EE%) of aripiprazole-loaded LLCNPs at a constant citrem/SPC ratio of 1:1 (CS1:1) is shown in Fig. 2. Four different aripiprazole concentrations of 1.0, 2.0, 2.5, and 5.0 mg/mL have been selected for this study. The results demonstrated high EE% value of ~92% for all understudied drug-loaded nanodispersions and was relatively independent of aripiprazole concentrations. This finding evidences the

possibility of LLCNPs to improve the encapsulation of poorly water-soluble aripiprazole as compared to other reported techniques such as using poly (lactic-co-glycolic acid) (PLGA) nanoparticles which the EE% values ranged from 20–40% only (Babu et al., 2014). Statistical analysis revealed that the mean score of citrem/SPC-loaded aripiprazole at the concentrations of 2.0, 2.5, and 5.0 mg/mL was significantly different ($p > 0.005$) compared to that of formulation with 1.0 mg/mL aripiprazole. Thus, the high EE% of aripiprazole into the LLCNPs indicates maximum amount of the drugs that have been successfully loaded into the LLCNPs.

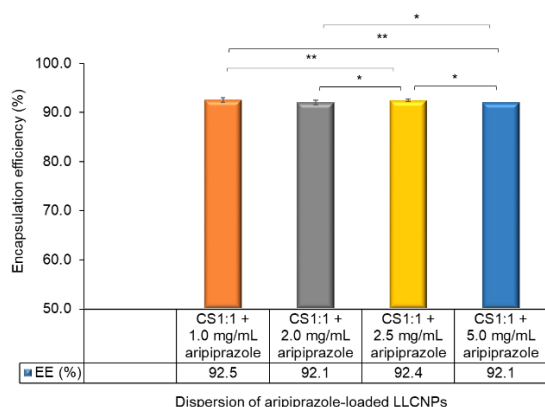


Fig. 2. Encapsulation efficiency (EE%) of aripiprazole-loaded binary mixture of citrem/SPC LLCNPs. Data are expressed as mean (one independent experiment). Results were analyzed by one sample *t*-test. The means marked with * and ** are significantly different with *p* value less than 0.05 and 0.01, respectively, as compared among the tested formulations.

3.1.1 Stability Study for Encapsulation Efficiency of Drug-Loaded LLCNPs

Fig. 3 shows the stability study for different concentrations of aripiprazole-loaded LLCNPs (1.0, 2.0, 2.5, and 5.0 mg/mL) through 5 days of storage at 4°C. Stability test of nanodispersions for several days were done in the lab to endure the stability of drugs in the body system while modulating their physicochemical and biological properties (Silki and Ranjan, 2018). The stability of encapsulated drug was attempted to analyze the presence of any metastable formulations in the batches so that we can obtain a stable formulation to be used for a longer duration (Khumbhar et al., 2021). From Fig. 3, formulation with 1.0 mg/mL aripiprazole showed a decreased value from 92.5 to 88.8% with total reduction of 3.7% within 5 days of storage. On the other hand, formulation with 2.0 mg/mL aripiprazole displayed better stability with a reduction of 1.6% from 92.1% to 90.5%. Similar total reduction was observed for the stability of formulation with 2.5 mg/mL aripiprazole (Fig. 3). The highest concentration of 5.0 mg/mL aripiprazole-loaded LLCNPs exhibited the least drug lost

with total reduction of only 1.0% from 92.0 to 91.0%. In overall, the 1.0 mg/mL of aripiprazole-loaded LLCNPs was relatively unstable compared to the other three nanodispersions that showed minimal drug lost. It can be observed that as the concentration of aripiprazole increases, the stability of encapsulated drug increases as well. Statistical analysis revealed that the mean score for EE% stability within 5 days of storage among the four aripiprazole-loaded LLCNPs showed no significant different ($p < 0.005$).

Hydrophobic interaction between phospholipid bilayer of SPC increases with increasing amount of aripiprazole (Babu et al., 2014). The high hydrophobic interaction will cause the drug to diffuse at a slower rate from the bilayer to the outer aqueous phosphate buffered saline medium (Babu et al., 2014). LLCNPs have a hydrophobic core that can encapsulate aripiprazole and a hydrophilic part that acts as an outer corona on lipid bilayers (Piazzini et al., 2020). This type of drug delivery system may extend the duration of the drug nanocarrier travels in the blood circulation (Piazzini et al., 2020) and thus, offers larger drug loading capacity across the blood brain barrier (Cagel et al., 2017; Piazzini et al., 2020).

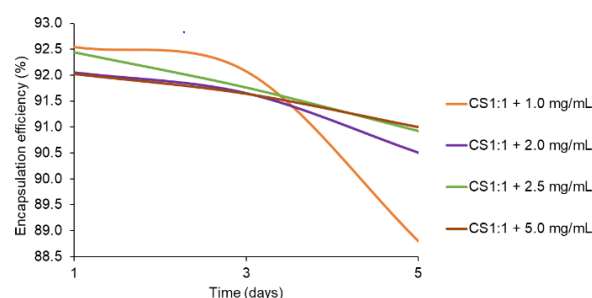


Fig. 3. Total drug lost (%) upon incubation storage for different drug-loaded concentrations. Data are expressed as mean (one independent experiment). Results were analyzed by one-way ANOVA.

3.2 Optimization of Drug-Free and Drug-Loaded LLCNPs

3.2.1 Particle Size, Zeta Potential, And Polydispersity Index Characterization for Drug-Free LLCNPs

The particle size, zeta potential, and polydispersity index (PDI) of the nanodispersions were assessed by dynamic light scattering. Fig. 4 shows the sonication time, particle size, zeta potential, and PDI of the drug-free LLCNPs prepared at two different sonication powers of 20 and 50%.

After 30 min of 20% sonication power, the particle size obtained was 475 nm with high PDI of 0.50 which indicates non-homogeneous particles size (Fig. 4(a) and 4(c)). Increasing the time to 60 min successfully reduced the particle size to 149 nm with low PDI of 0.11 (Fig. 4(a) and 4(c)) denoting a homogenous particle size was attained.

Danaei and co-workers (2018) stated that a PDI value of 0.30 or less was desirable, implying a relatively homogeneous formulation (Danaei et al., 2018). Herein, the zeta potential values of all the prepared nanodispersions were negatively-charged (Fig. 4(b)). Such a tendency could be attributed to the presence of the negatively-charged head group of the citrem (Azmi et al., 2016). In principle, zeta potential values above +30 mV or below -30 mV provide a good stability in the dispersion medium (Gabr et al., 2017). As shown in Fig. 4(b), all zeta potentials after sonication were recorded with a magnitude lower than 30 mV implying electrostatic force of attraction between nanoparticles exceeds the repulsion force. Specifically, increasing the sonication time to 60 min further reduced the negative zeta potential value, thus signifying lack of colloidal stability compared to that of 30 min sonication time (Fig. 4(b)). Nonetheless, both mean particle size and PDI of the drug-free LLCNPs at 60 min still demonstrates relatively good homogenous formulation compared to the 30 min sonication period. However, 20% sonication power at 60 min was consider as time-consuming process for the preparation of stable and well-dispersed milky formulation. Therefore, the method was optimized to higher sonication power (50%) but with shorter time interval (5, 7, 10, and 13 min).

Using 50% sonication power at different time intervals of 5, 7, 10, and 13 min, all drug-free LLCNPs produced particle sizes of less than 167 nm with small PDIs of less than 0.30 implying the homogeneous particle size distribution were formed. Different sonication times ranging from 5 to 13 min were studied since they can impact the dispersion behaviors and aggregation size of nanoparticles (Mahbubul et al., 2015). The zeta potential for drug-free LLCNPs prepared through sonication for 5 min was -26.3 mV (Fig. 4(b)). At longer sonication time of 7, 10,

and 13 min, the negative zeta potential showed slightly different values from -26.1 to -23.1 mV (Fig. 4(b)). Smaller particle size and homogenous formulations were achieved upon longer sonication time. The particle size for 5 min sonication time was 166 nm with PDI of 0.27 (Fig. 4(a) and 4(c)), whereas for 7 min sonication time, the particle size was 152 nm with PDI of 0.21 (Fig. 4(a) and 4(c)). Sonication time of 10 min formed particle size of 154 nm with PDI of 0.17 (Fig. 4(a) and 4(c)). The optimized condition was obtained at 13 min sonication time which gave particle size of 150 nm with PDI of 0.13 (Fig. 4(a) and 4(c)). Statistical analysis revealed that the mean score of particle size, PDI, and zeta potential for citrem/SPC-loaded aripiprazole at the concentration of 2.0 and 2.5 mg/mL including the drug-free nanodispersion showed no significant different ($p < 0.005$) in comparison between group.

Based on the findings, the particle size, polydispersity index, and zeta potential of drug-free LLCNPs decreased as the time for sonication increased indicate less stable nanodispersions. The decrease in particle size and PDI was due to sufficient energy to break the particle into smaller parts and evenly distributed in the aqueous medium (Olson, n.d.; Uner, 2006; Larsson et al., 2012). The decreased negative zeta potential implies less stabilization of the nanodispersions due to the lack of electrostatic force of repulsion between particles (Gabr et al., 2017). Thus, 10 min of 50% power of sonication was selected as the optimum condition to prepare the drug-free and drug-loaded LLCNPs because the differences in particles size, polydispersity index and zeta potential between 10 and 13 min of sonication time shows no differences in the stability of nanoparticles.

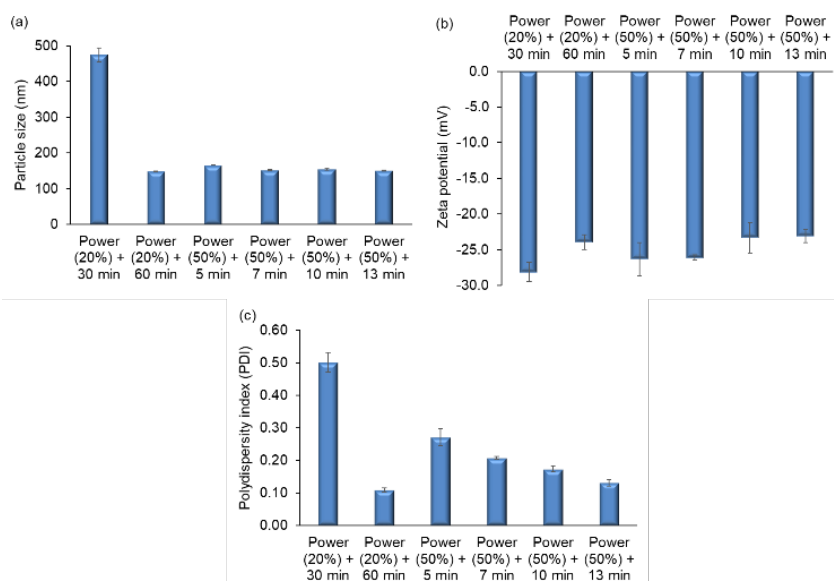


Fig. 4. Optimization conditions via different sonication time and power based on dynamic light scattering analysis involving (a) particle size, (b) zeta potential, and (c) PDI of drug-free LLCNPs. Data are expressed as mean \pm SD of triplicates (one independent experiment). Results were analyzed by one-way ANOVA.

3.2.2 Particle Size, Zeta Potential, and PDI for Drug-Loaded LLCNPs Upon Storage Conditions

Using the optimized method obtained (from subsection 3.2.1), the particle size, zeta potential, and PDI values of drug-free and drug-loaded LLCNPs are summarized in Table 1. Since the value of EE% (Fig. 2) was not improved for aripiprazole concentration higher than 2.5 mg/mL, thus 5.0 mg/mL aripiprazole-loaded LLCNPs was not considered for additional stability study upon incubation. The particle size of drug-free LLCNPs obtained was 154 nm with PDI of 0.17. Loading 1.0 mg/mL of aripiprazole into LLCNPs gave an increment of particle size to 161 nm with PDI of 0.11. Meanwhile, LLCNPs loaded with 2.0 mg/mL and 2.5 mg/mL of aripiprazole resulted in larger particle size of 186 nm (PDI of 0.16) and 183 nm (PDI of 0.10), respectively. On the other hand, the zeta potentials of drug-free LLCNPs, 1.0, 2.0, and 2.5 mg/mL of aripiprazole-loaded LLCNPs were recorded within a range of -21.5 to -

23.8 mV. In general, the LLCNPs prepared for both drug-free and drug-loaded were below 186 nm, with PDI less than 0.30. The value of negative zeta potentials of the drug-free and drug-loaded LLCNPs are acceptable, thus implying small particles size with homogenous particle size distribution of LLCNPs were formed.

Upon storage, the changes in particle size, zeta potential, and PDI of drug-free and drug-loaded LLCNPs were illustrated in Fig. 5. For drug-free LLCNPs, the particle size increased from 154 to 404 nm with PDI increased from 0.17 to 0.51 after 17 days (Fig. 5(a) and (c)). The negative zeta potential value also increased in magnitude from -23.3 to -27.8 mV indicating an improved electrostatic stabilization of the nanoparticles (Figure 5(b)). Significant changes in particle size and zeta potential were also obtained with aripiprazole-loaded LLCNPs. The 1.0 mg/mL of aripiprazole-loaded LLCNPs showed an increment in the particle size (from 161 to 1414 nm) as well as the PDI (from 0.11 to 0.91) as the storage time increases (Fig. 5(a) and (c)).

Table 1. Particle size, zeta potential, and PDI of drug-free and drug-loaded LLCNPs upon 17 days of storage. Data are expressed as mean ± SD of triplicates (one independent experiment)

Sample	Particle size (nm)			Zeta potential (mV)			PDI		
	Day 1	Day 9	Day 17	Day 1	Day 9	Day 17	Day 1	Day 9	Day 17
CS1:1 (drug-free)	154 ± 2	247 ± 3	404 ± 14	-23.3 ± 2.1	-25.4 ± 2.0	-27.8 ± 2.3	0.17 ± 0.01	0.17 ± 0.02	0.51 ± 0.02
CS1:1 + 1.0 mg/mL aripiprazole	161 ± 1	464 ± 8	1414 ± 165	-21.5 ± 1.2	-23.7 ± 1.0	-29.1 ± 2.0	0.11 ± 0.02	0.51 ± 0.01	0.91 ± 0.01
CS1:1 + 2.0 mg/mL aripiprazole	186 ± 2	784 ± 70	630 ± 82	-23.8 ± 1.8	-27.4 ± 2.1	-28.3 ± 0.1	0.16 ± 0.01	0.62 ± 0.01	0.56 ± 0.02
CS1:1 + 2.5 mg/mL aripiprazole	183 ± 1	522 ± 24	349 ± 4	-22.9 ± 1.0	-26.0 ± 0.4	-26.5 ± 3.4	0.10 ± 0.01	0.44 ± 0.05	0.42 ± 0.05

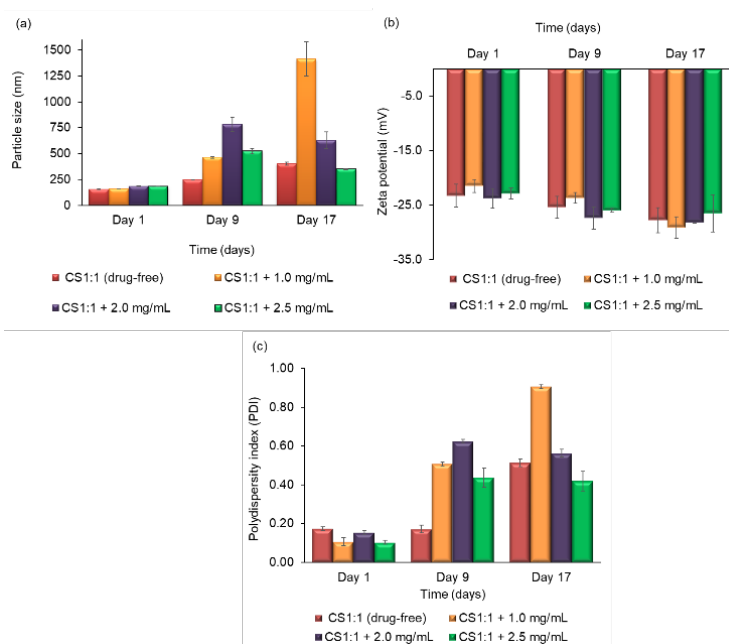


Fig. 5. Stability analysis of (a) particle size, (b) zeta potential, and (c) PDI using dynamic light scattering analysis. Data are expressed as mean ± SD of triplicates (one independent experiment). Results were analyzed by one-way ANOVA.

The corresponding negative zeta potential was increased from -21.5 to -29.1 mV (Fig. 5(b)). As for 2.0 mg/mL of aripiprazole-loaded LLCNPs, the particle size was elevated from 186 to 784 nm with PDI raised up from 0.16 to 0.62 upon 9 days of storage. However, after 17 days of storage, we observed a decrease in both particle size and PDI values from 784 to 630 nm and 0.62 to 0.56, respectively (Fig. 5(a) and (c)). On the other hand, the corresponding negative zeta potential value was increased from -23.8 to -28.3 mV as the storage time increases up to 17 days (Fig. 5(b)). The 2.5 mg/mL of aripiprazole-loaded LLCNPs exhibited similar trend as the 2.0 mg/mL aripiprazole concentration for the particle size (Fig. 5(a)), zeta potential (Fig. 5(b)), and PDI (Fig. 5(c)) values. Such observation for high drug concentrations could be explained by physical and chemical instability of cubosome nanoparticles (Fig. 6), which often synthesized in solution as colloidal systems and cannot be kept for lengthy periods of time (Malheiros et al., 2021). As a result, it is critical to investigate alternative storage settings for cubosomes in order to extend their shelf life (e.g. freeze drying method) (Malheiros et al., 2021). Some processes are employed in the pharmaceutical industry to improve the stability of a given formulation (Malheiros et al., 2021). Statistical analysis revealed that the mean score for stability study of particle size, PDI, and zeta potential over 17 days among drug-free and drug-loaded LLCNPs at the concentration of 1.0, 2.0, and 2.5 mg/mL showed no significant different ($p < 0.005$) in comparison between group.

The 2-week storage stability of aripiprazole-loaded LLCNPs after optimization is crucial for future applications as it is related to the electrostatic charge of nanoparticles (Luangtana-Anan et al., 2010; Cai et al., 2017). The increase in both particle size and PDI of the drug-free and 1.0 mg/mL of aripiprazole loaded LLCNPs was probably due to the occurrence of coalescent between LLCNPs. This causes them to aggregate and become bigger in particle sizes whilst their steric stabilization was sufficient to keep them together.

3.3 Structural Characterization of Drug-Loaded LLCNPs

Binary citrem/SPC (CS1:1) mixtures of drug-free and loaded-aripiprazole of different drug concentrations listed in Table 2 were characterized by small-angle X-ray scattering (SAXS). An internal inverse hexagonal (H_2) phase (or known as hexosomes) with reciprocal spacing ratios of $\sqrt{1}$, $\sqrt{3}$, and $\sqrt{4}$ was observed for all formulations in Fig. 6. The internal nanostructure of these nanodispersions was retained with almost similar lattice parameter as the aripiprazole concentration increases (Table 2). It is suggested that the asymmetric insertion of citrem occurs through preferential charged-dipole interactions between the positively charged choline group of the zwitterionic headgroups of SPC molecules and the anionic moieties of citrem resulted in the stabilization of this curved state of asymmetric bilayers (Azmi et al., 2016).

Table 2. Internal nanostructures of drug-free and drug-loaded nanodispersions at citrem/SPC [1:1] measured by SAXS

LLCNPs	Internal nanostructure	Lattice parameter (nm)
CS1:1 (drug-free)	H_2 phase	6.96
1.0 mg/mL aripiprazole	H_2 phase	6.90
2.0 mg/mL aripiprazole	H_2 phase	6.84
2.5 mg/mL aripiprazole	H_2 phase	6.83

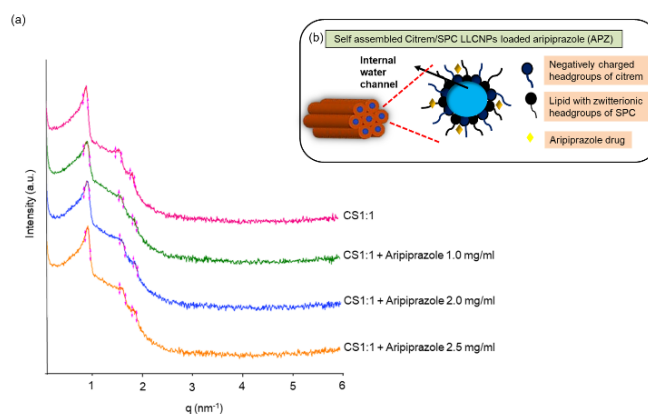


Fig. 6. Structural characterization of drug-free and drug-loaded LLCNPs at three different concentrations (a) SAXS diffractograms, performed at 25°C. The intensities have been shifted by a constant arbitrary factor for better visibility and (b) conceptual scheme of aripiprazole-loaded LLCNPs. Example is shown as internal inverse hexagonal (H_2) nanostructures.

3.4 Morphological Characterization of Drug-Free and Drug-Loaded LLCNPs

Transmission electron microscopy (TEM) was used to observe the morphological and the distribution of LLCNPs. The drug-free and aripiprazole-loaded LLCNPs at low (Figs. 7(a) and 8(a)) and high (Figs. 7(b) and 8(b)) magnifications were obtained. The morphology results for both formulations were in a good agreement with SAXS analysis of inversed type LLCNPs. The occurrence of internal nanostructure of H_2 phase was observed at higher magnification. Interestingly, aripiprazole-loaded LLCNPs illustrated more closely packed formation of lipid bilayers, thus indicated significant interaction between aripiprazole and lipid bilayers formed by SPC and citrem. Since aripiprazole is a poorly water-soluble drug with limited solubility, it is relatively hydrophobic and showed good affinity towards the lipid bilayer formed by SPC. This induced an interaction through van der Waals forces (Chong et al., 2015). The interaction is therefore, maintained the internal nanostructure of H_2 phase with slightly smaller aqueous nanochannels (Fig. 6).

3.5 Fourier Transform Infrared Spectroscopy Analysis

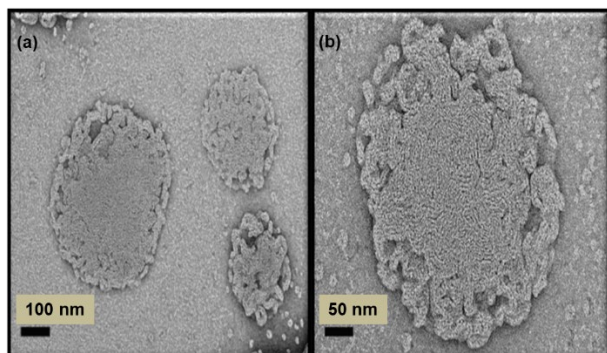


Fig. 7. TEM image showing the morphology of drug-free LLCNPs at (a) low and (b) high magnifications

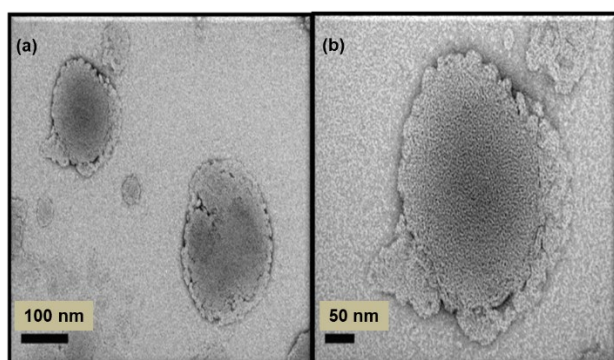


Fig. 8. TEM image showing the morphology of aripiprazole-loaded LLCNPs at (a) low and (b) high magnifications

3.5.1 Ftir Spectra of Aripiprazole

The FTIR spectra of aripiprazole, drug-free, and drug-loaded LLCNPs are presented in Fig. 9. The FTIR spectrum of aripiprazole (Fig. 9(a)) displayed an absorption band at 3472/cm indicated the N-H stretching of the secondary amide group of the lactam ring. Aromatic stretching = C-H vibration showed two absorption bands at 3103 and 3063/cm (Stuart, 2004; Ardiana et al., 2013; Begam et al., 2014). The absorption band at 1375/cm corresponded to the C-N stretching vibration of the aromatic amine (Stuart, 2004; Ardiana et al., 2013; Begam et al., 2014). Aromatic = C-Cl out of plane bending vibration showed a strong absorption band at 78/cm. This peak also indicated the *ortho*-substituted chloride in the benzene ring (Stuart, 2004; Ardiana et al., 2013; Begam et al., 2014). The peak at 675/cm is due to the out of plane vibration of N-H of the secondary amide group (Stuart, 2004; Ardiana et al., 2013; Begam et al., 2014). While absorption bands in the region of 407–591/cm are attributed to C-C-C out of plane bending vibration of the alkyl chain (Stuart, 2004; Ardiana et al., 2013; Begam et al., 2014).

In the FTIR spectrum of drug-free LLCNPs (Fig. 9(b)), the absorption band at 3221/cm belongs to O-H stretching of carboxylic acid, citric acid and glycerol (Stuart, 2004; Ardiana et al., 2013; Begam et al., 2014). Typical peaks around 2959–2868/cm corresponded to the stretching

vibration of alkyl groups (CH₂) of phospholipids. A strong absorption at the 1158/cm indicated the presence of C-O stretching vibration of carboxylic acid O = C-OH. It also may be due to the P = O stretching vibration of the phosphate group of soy phosphatidylcholine (Stuart, 2004; Ardiana et al., 2013; Begam et al., 2014). The peak at 1059/cm corresponded the symmetric stretching vibration of the C-O-C of ester bond (Stuart, 2004; Ardiana et al., 2013; Begam et al., 2014). The absorption band observed at 943/cm belongs to the asymmetric stretching vibration of P-O-C, while that at 854/cm can be attributed to symmetric stretching vibration of P-O-C of the bond formed between phosphate group and glycerol (Stuart, 2004; Ardiana et al., 2013; Begam et al., 2014). Absorption band of 739/cm was from C-C-OH out of plane bending of alcohol like in citrate or glycerol (Stuart, 2004; Ardiana et al., 2013; Begam et al., 2014).

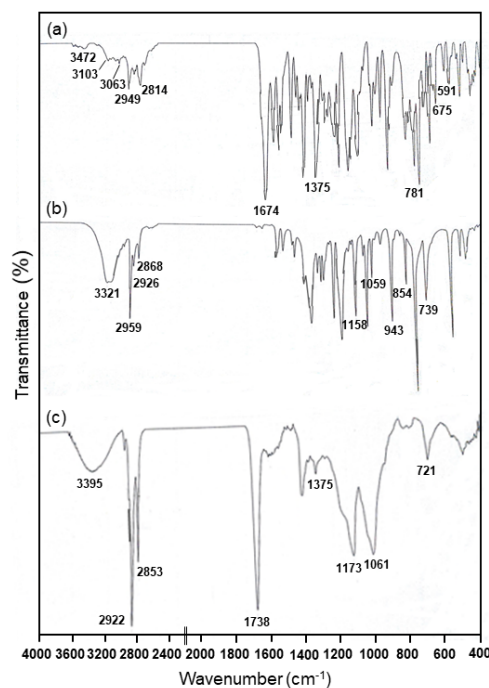


Fig. 9. FTIR spectra of (a) pure aripiprazole, (b) drug-free, and (c) aripiprazole-loaded LLCNPs

For drug-loaded LLCNPs (Fig. 9(c)), the peak located at 2922 and 2853/cm (CH₂) was similar to that of drug-free LLCNPs. The O-H stretching band at 3221/cm was shifted to 3395/cm which suggested some interaction by intermolecular hydrogen bonds. The band for C-N stretching vibration of aromatic amine in aripiprazole (1375/cm) became reduced in intensity in the drug-loaded LLCNPs. This suggested that aripiprazole was entrapped within the LLCNPs, possibly by hydrophobic interactions.

3.6 Thermal Properties

Fig. 10 illustrates the DSC thermograms of aripiprazole,

SPC, drug-free, and drug-loaded LLCNPs. Three endothermic peaks of aripiprazole were detected at 89, 140, and 149°C corresponding to its melting points for the different crystal forms (Fig. 10(a)). In general, the DSC curve of aripiprazole could be divided into two regions: (i) below 130°C is the dehydration/melting of hydrate form and (ii) above 130°C is the melting of anhydrous form (Ayala et al., 2010). The peak at 140°C is typically associated with the melting of the anhydrous form, while the observation of another melting point at 149°C evidenced the phase transition to another crystal form during the heating process. SPC thermogram disclosed three endothermic peaks at 97, 190, and 263°C which are correlated with its liquid crystalline nature (Fig. 10(b)). The first phase transition occurred at 97°C corresponding to the change from ordered gel phase to less ordered crystalline phase (planar gel). The second phase transition was observed at 190°C indicating transition to a new crystalline phase (rippled phase), while the third phase transition at 263°C signifies the transition to lamellar liquid crystalline phase Popova and Hinch, 2011).

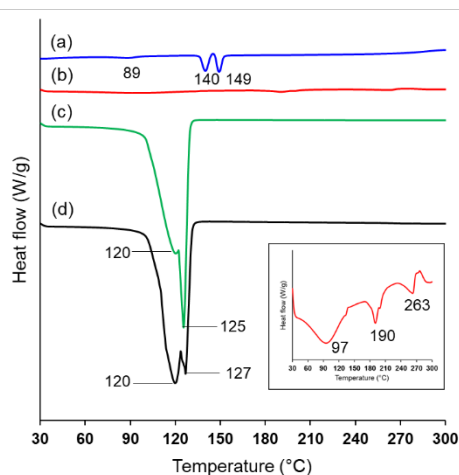


Fig. 10. DSC thermograms of (a) aripiprazole, (b) SPC, (c) drug-free, and (d) aripiprazole-loaded LLCNPs. The inset shows a larger scale of SPC thermogram. The heat flows have been shifted by a constant arbitrary factor for better visibility.

As expected, the DSC thermograms of both drug-free (Fig. 10(c)) and drug-loaded (Fig. 10(d)) LLCNPs experienced different endothermic event from those of aripiprazole and SPC which implies the formation of a new structure with different thermal characteristics. For drug-free LLCNPs, a double peak was observed at 120 and 125°C, while for drug-loaded LLCNPs, a double peak was detected at 120 and 127°C. Their peaks appeared to be broader than the pure aripiprazole and SPC due to the particles size distribution of the nanoparticles (Longo et al., 2011). A slight shift towards higher temperature value in case of drug-loaded LLCNPs than drug-free LLCNPs suggests an interaction between aripiprazole and the binary mixture of citrem/SPC. Moreover, the absence of aripiprazole

endothermic peaks in the thermogram of drug-loaded LLCNPs implies that aripiprazole was well encapsulated within the nanodispersion.

3.7 *In Vitro* Drug Release Profile of Drug-Loaded LLCNPs

The drug release study for the 2.5 mg/mL of aripiprazole-loaded LLCNPs in Fig. 11 shows a sustained release profile up to 96 h. More than 50 and 70% of aripiprazole were released from LLCNPs after 24 and 48 h, respectively. After 96 h, around 97% of aripiprazole was released from the nanodispersion. The sustained release rate of LLCNPs is possibly due to the interaction of the drug with the lipidic bilayer (Kumar et al., 2007). Previously, Babu and co-workers (2014) reported the aripiprazole release study from PLGA nanoparticles up to 35 days with 80% of the drug was released out but with limited encapsulation efficiency (Babu et al., 2014). Additionally, the *in vitro* release data was in a good agreement with the stability result for 2.5 mg/mL of aripiprazole-loaded LLCNPs in which this inverted typed LLCNPs offer an exceptional long-term stability of particle size, zeta potential, and PDI with excellent drug encapsulation efficiency Table 1 and Fig. 2).

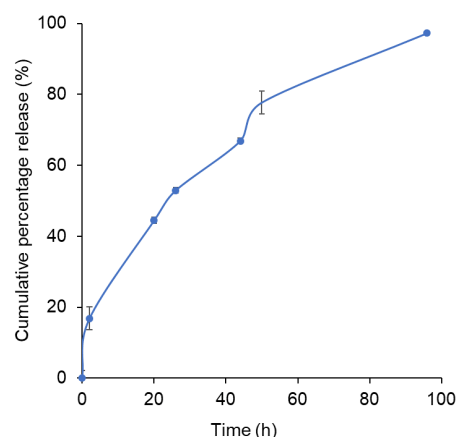


Fig. 11. *In vitro* release profile for 2.5 mg/mL of aripiprazole-loaded LLCNPs

4. CONCLUSION

An inverted type LLCNPs was successfully prepared using a binary mixture of SPC and citrem-loaded with aripiprazole. The EE% of aripiprazole-loaded LLCNPs was relatively high (92%) with all formulations at different drug concentrations (1.0, 2.0, 2.5, and 5.0 mg/mL). The optimized method of preparation using high-energy ultrasonication method at 50% power of sonication, was significantly efficient to form homogenous solution in 10 min. The particles size for the drug-free and drug-loaded LLCNPs (1.0 to 2.5 mg/mL) was in the range of 154 to 186 nm, PDI from 0.10 to 0.17 and negative zeta potential around -21.5 to -23.8 mV. The stability studies up to 17 days

of incubation period, resulted in coalescent between LLCNPs causing them to aggregate and become larger particles. However, the steric stabilization from zeta potential of LLCNPs was improved. Based on the SAXS and TEM analysis, an inverse hexagonal (H₂) phase LLCNPs was observed. An interaction between aripiprazole with SPC and citrem was also observed from the FTIR and DSC results. The drug release from 2.5 mg/mL of aripiprazole-loaded LLCNPs revealed sustained release performance up to 96 h. In conclusion, this study proposed the promising usage of inversed type LLCNPs as a potential nanocarrier for aripiprazole delivery, which is projected to enhance the drug encapsulation and sustained release of this drug-loaded LLCNPs upon administration to a living organism. However, biological studies such as an in vitro toxicity study for aripiprazole-loaded LLCNPs should be further investigated to ensure its biocompatibility and efficacy with the related cells.

ACKNOWLEDGMENT

The authors would like to extend their sincere appreciation to the Ministry of Education (MOE) Malaysia for funding this research through Fundamental Research Grant Scheme (FRGS/1/2018/STG07/UPM/02/4) and Geran Putra UPM (9589800).

CONFLICT OF INTEREST

The authors declare that they have no conflict of interest.

REFERENCES

- Akbarzadeh, A., Rezaei-Sadabady, R., Davaran, S., Joo, S.W., Zarghami, N., Hanifehpour, Y., Samiei, M., Kouhi, M., Nejati-Koshki, K. 2013. Liposome: classification, preparation, and applications. *Nanoscale Research Letters*, 8, 102.
- Ardiana, F., Lestari, M.L.A.D., Indrayanto, G. 2013. Aripiprazole: In profiles of drug substances, excipients and related methodology, 38, 2–501.
- Asha Spandana, A.K.M., Natarajan, J., Thirumaleshwar, S., Hemanth Kumar, S. 2020. A review of the preparation, characterization and application of nanostructured lipid carriers. *International Journal of Research in Pharmaceutical Sciences*, 11, 1130–1135.
- Ayala, A.P., Honorato, S.B., Filho, J.M., Grillo, D., Quintero, M., Gilles, F., Polla, G. 2010. Thermal stability of aripiprazole monohydrate investigated by raman spectroscopy. *Vibrational Spectroscopy*, 54, 169–173.
- Azmi, I.D.M., Wibroe, P.P., Wu, L.P., Kazem, A.I., Amenitsch, H., Moghimi, S.M., Yagmur, A. 2016. A structurally diverse library of safe-by-design citrem-phospholipid lamellar and non-lamellar liquid crystalline nano-assemblies. *Journal of Controlled Release*, 239, 1–9.
- Babu, C., Kumara Babu, P., Sudhakar, K., Subha, M.C.S., Chowdoji Rao, K. 2014. Aripiprazole-loaded PLGA nanoparticles for controlled release studies: Effect of co-polymer ratio. *International Journal of Drug Delivery*, 6, 151–155.
- Badr-Eldin, S.M., Ahmed, T.A., Ismail, H.R. 2013. Aripiprazole-cyclodextrin binary systems for dissolution enhancement: Effect of preparation technique, cyclodextrin type and molar ratio. *Iranian Journal of Basic Medical Sciences*, 16, 1223–1231.
- Bastos, M. 2016. Using DSC to characterize thermotropic phase transitions in lipid bilayer membranes: The basics of liposome sample preparation and DSC studies. Malvern Instruments Limited, 1–21.
- Begam, M., Datta, V.M., Gowda, D.V., Aravindaram, A.S., Siddaramiah. 2014. Development and characterization of co-ground mixtures and solid dispersions of aripiprazole with hydrophilic carriers. *International Journal of Pharmacy and Pharmaceutical Sciences*, 6, 552–557.
- Bhosale, R., Osmani, R.A., Harkare, B.R., Ghodake, P.P. 2013. Cubosomes: The inimitable nanoparticulate drug carriers. *Scholars Academic Journal of Pharmacy*, 2, 481–486.
- Bonate, P.L. 2011. Pharmacokinetics. *Wiley Interdisciplinary Reviews: Computational Statistics*, 3, 332–342.
- Braun, D.E., Gelbrich, T., Kahlenberg, V., Tessadri, R., Wieser, J., Griesser, U.J. 2009. Conformational polymorphism in aripiprazole: preparation, stability and structure of five modifications. *Journal of Pharmaceutical Sciences*, 98, 2010–2026.
- Cagel, M., Tesan, F.C., Bernabeu, E., Salgueiro, M.J., Zubillaga, M.B., Moreton, M.A., Chiappetta, D.A. 2017. Polymeric mixed micelles as nanomedicines: Achievements and perspectives. *European Journal of Pharmaceutics and Biopharmaceutics*, 113, 211–228.
- Cai, L., Lin, C., Yang, N., Huang, Z., Miao, S., Chen, X., Pan, J., Rao, P., Liu, S. 2017. Preparation and characterization of nanoparticles made from co-incubation of SOD and glucose. *Nanomaterials*, 7, 1–11.
- Cerpnjak, K., Zvonar, A., Gasperlin, M., Vrecer, F. 2013. Lipid based system as a promising approach for enhancing the bioavailability of poor water-soluble drugs. *Acta Pharmaceutica*, 63, 427–445.
- Chandrashekar V.K. 2012. Lipid crystallization: From self-assembly to hierarchical and biological ordering. *Nanoscale*, 4, 5779–5791.
- Chime, S.A. Onyishi, I.V. 2013. Lipid-based drug delivery systems (LDDS): Recent advances and applications of lipids in drug delivery. *African Journal of Pharmacy and Pharmacology*, 7, 3034–3059.
- Chong, J.Y.T., Mulet, X., Boyd, B.J., Drummond, C.J. 2015. Steric stabilizers for cubic phase lyotropic liquid crystal nanodispersions (cubosomes). In *Advances in Planar Lipid Bilayers and Liposomes*, 21, 131–187.

- Chountoulesi, M., Perinelli, D.R., Forsys, A., Trzebicka, B., Pispas, S., Demetzos, C. 2020. Liquid crystalline nanoparticles for drug delivery: the role of gradient and block copolymers on the morphology, internal organization and release profile. *European Journal of Pharmaceutics and Biopharmaceutics*, 1–62.
- Chountoulesi, M., Pippa, N., Pispas, S., Chrysina, E.D., Forsys, A., Trzebicka, B., Demetzos, C. 2018. Cubic lyotropic liquid crystals as drug delivery carriers: Physicochemical and morphological studies. *International Journal of Pharmaceutics*, 550, 57–70.
- Dutta, L., Mukherjee, B., Chakraborty, T., Das, M.K., Mondal, L., Bhattacharya, S., Gaonkar, R.H., Debnath, M. C. 2018. Lipid-based nanocarrier efficiently delivers highly water soluble drug across the blood–brain barrier into brain. *Drug Delivery*, 25, 504–516.
- Elezaby, R.S., Gad, H.A., Metwally, A.A., Geneidi, A.S., Awad, G.A. 2017. Self-assembled amphiphilic core-shell nanocarriers in line with the modern strategies for brain delivery. *Journal of Controlled Release*, 261, 43–61.
- Gabr, M.M., Mortada, S.M., Sallam, M.A. 2017. Hexagonal liquid crystalline nanodispersions proven superiority for enhanced oral delivery of rosuvastatin: In vitro characterization and in vivo pharmacokinetic study. *Journal of Pharmaceutical Sciences*, 106, 3103–3112.
- Guo, C., Wang, J., Cao, F., Lee, R.J., Zai, G. 2010. Lyotropic liquid crystal systems in drug delivery. *Drug Delivery Today*, 15, 1032–1040.
- Huang, Y., Gui, S. 2018. Factors affecting the structure of lyotropic liquid crystals and the correlation between structure and drug diffusion. *RSC Advances*, 8, 6978–6987.
- Huang, Y., Gui, S. 2018. Factors affecting the structure of lyotropic liquid crystals and the correlation between structure and drug diffusion. *RSC Advances*, 8, 6978–6987.
- Kalepu, S., Nekkanti, V. 2015. Insoluble drug delivery strategies: review of recent advances and business prospects. *Acta Pharmaceutica Sinica B*, 5, 442–453.
- Khani, S., Keyhanfar, F., Amani, A. 2016. Design and evaluation of oral nanoemulsion drug delivery system of mebupine, *Drug Delivery*, 23, 2035–2043.
- Krishna Sailaja, A., Amareshwar, P., Chakravarty, P. 2011. Formulation of solid lipid nanoparticles and their applications. *Current Pharma Research*, 1, 197–203.
- Kumar, A., Singh, H., Mishra, A., Mishra, A.K. 2020. Aripiprazole: An FDA Approved bioactive compound to treat schizophrenia- A mini review. *Current Drug Discovery Technologies*, 17, 23–29.
- Kumar, V.V., Chandrasekar, D., Ramakrishna, S., Kishan, V., Rao, Y.M., Diwan, P.V. 2007. Development and evaluation of nitrendipine loaded solid lipid nanoparticles: Influence of wax and glyceride lipids on plasma pharmacokinetics. *International Journal of Pharmaceutics*, 335, 167–175.
- Kumbhar, S.A., Kokare, C.R., Shrivastava, B., Gorain, B., Choudhury, H. 2021. Antipsychotic potential and safety profile of TPGS-based mucoadhesive aripiprazole nanoemulsion: Development and optimization for nose-to-brain delivery. *Journal of Pharmaceutical Sciences*, 110, 1761–1778.
- Larsson, M., Hill, A., Duffy, J. 2012. Suspension stability: Why particle size, zeta potential and rheology are important. *Annual Transactions of the Nordic Rheology Society*, 20, 209–214.
- Lertxundi, U., Hernandez, R., Medrano, J., Domingo-Echaburu, S., Garcia, M., Aguirre, C. 2018. Aripiprazole and impulse control disorders: Higher risk with the intramuscular depot formulation? *International Clinical Psychopharmacology*, 33, 56–58.
- Liu, K., Feng, Z., Shan, L., Yang, T., Qin, M., Tang, J., Zhang, W. 2017. Preparation, characterization, and antioxidative activity of *bletilla striata* polysaccharide/chitosan microspheres for oligomeric proanthocyanidins. *Drying Technology*, 35, 1629–1643.
- Longo, A., Carotenuto, G., Palomba, M., De Nicola, S. 2011. Dependence of optical and microstructure properties of thiol-capped silver nanoparticles embedded in polymeric matrix. *Polymers*, 3, 1794–1804.
- Luangtana-Anan, M., Limmatvapirat, S., Nunthanid, J., Chalongsuk, R., Yamamoto, K. 2010. Polyethylene glycol on stability of chitosan micro-particulate carrier for protein. *AAPS Pharm SciTech*, 11, 1376–1382.
- Mahbulbul, I.M., Saidur, R., Amalina, M.A., Elcioglu, E.B., Okutucu-Ozyurt, T. 2015. Effective ultrasonication process for better colloidal dispersion of nanofluid. *Ultrasonic Sonochemistry*, 26, 361–369.
- Malheiros, B., Dias de Castro, R., Lotierzo, M.C.G., Casadei, B.R., Barbosa, L.R.S. 2021. Design and manufacturing of monodisperse and malleable phytantriol-based cubosomes for drug delivery applications. *Journal of Drug Delivery Science and Technology*, 61, 102149.
- Maslizan, M., Azmi, I.D.M., Jaafar, A.M., Haris, M.S. 2021. Nanotechnology for molecular imaging of atherosclerosis: Current design and approaches. *Journal of Advanced Research in Fluid Mechanics and Thermal Sciences*, 81, 124–138.
- Modi, S., Anderson, B.D. 2013. Determination of drug release kinetics from nanoparticles: Overcoming pitfalls of the dynamic dialysis method. *Molecular Pharmaceutics*, 10, 3076–3089.
- Nethravani, G., Kishore Babu, M., Kalyani, V., Dakshinamurthy, D.V., Murali Krishna, G.V. 2014. Formulation and evaluation of aripiprazole-loaded liposomes for brain drug delivery. *Journal of Chemical and Pharmaceutical Sciences*, 7, 14–20.
- Olson, E. n.d. Zeta potential and colloidal chemistry. Particle Technology Labs, www.particletechlabs.com.
- Piazzini, V., Landucci, E., Urru, M., Chiarugi, A., Pellegrini-Giampietro, D.E., Bilia, A.R., Bergonzi, M.C. 2020. Enhanced dissolution, permeation and oral bioavailability of aripiprazole mixed micelles: In vitro

- and in vivo evaluation. *International Journal of Pharmaceutics*, 583, 119361.
- Popova, A.V., Hinch, D.K. 2011. Thermotropic phase behavior and headgroup interactions of the nonbilayer lipids phosphatidylethanolamine and monogalactosyldiacylglycerol in the dry state. *BMC Biophysics*, 4, 1–11.
- Saari, N.A.N., Mislan, A.A., Hashim, R., Zahid, N.I. 2018. Self-assembly, thermotropic, and lyotropic phase behavior of guerbet branched-chain maltosides. *Langmuir*, 34, 8962–8974.
- Savjani, K.T., Gajjar, A.K., Savjani, J.K. 2012. Drug solubility: Importance and enhancement techniques. *International Scholarly Research Network Pharmaceutics*, 1–10.
- Shirley, M., Perry, C.M. 2014. Aripiprazole (ABILIFY MAINTENA®): A review of its use as maintenance treatment for adult patients with schizophrenia. *Drugs*, 74, 1097–1110.
- Silki, Sinha, V.R. 2018. Enhancement of in vivo efficacy and oral bioavailability of aripiprazole with solid lipid nanoparticles. *AAPS Pharm SciTech*, 19, 1264–1273.
- Socrates, G. 2004. Infrared and raman characteristic group frequencies. *Journal of Raman Spectroscopy*, 35, 905.
- Spicer, P.T. 2004. Cubosomes: Bicontinuous liquid crystalline nanoparticles. *Dekker Encyclopedia of Nanoscience and Nanotechnology*, 881–892.
- Stuart, B.H. 2004. Infrared spectroscopy: Fundamentals and applications.
- Tan, A., Hong, L., Du, J.D., Boyd, B.J. 2018. Self-assembled nanostructured lipid systems: Is there a link between structure and cytotoxicity? *Advanced Science*, 6, 1–21.
- Thadanki, M., Kumari, P.S., Prabha, K.S. 2011. Overview of cubosomes: A nanoparticle. *International Journal of Research in Pharmacy and Chemistry*, 1, 535–541.
- Uner, M. 2006. Preparation, characterization and physico-chemical properties of Solid Lipid Nanoparticles (SLN) and Nanostructured Lipid Carriers (NLC): Their benefits as colloidal drug carrier system. *Pharmazie*, 61, 375–386.
- William, H.D., Trevaskis, N.L., Charman, S.A., Shanker, R.M., Charman, W.N., Pouton, C.W., Christopher J. H. Porter. 2013. Strategies to address low drug solubility in discovery and development. *Pharmacology Revision*, 65, 315–499.
- Xu, Y., Liu, X., Lian, R., Wu, W. 2012. Enhanced dissolution and oral bioavailability of aripiprazole nanosuspension prepared by nanoprecipitation/homogenization based on acid-base neutralization. *International Journal of Pharmaceutics*, 438, 287–295.
- Yaghmur, A., Mu, H. 2021. Recent advances in drug delivery applications of cubosomes, hexosomes, and solid lipid nanoparticles. *Acta Pharmaceutica Sinica B*, 11, 871–885.
- Zhai, J., Tran, N., Sarkar, S., Fong, C., Mulet, X., Drummond, C. 2017. Self-assembled lyotropic liquid crystalline phase behavior of monoolein-capric acid-phospholipid nanoparticulate systems. *Langmuir*, 33, 2571–2580.